



## ARCHIVIO ISTITUZIONALE DELLA RICERCA

### Alma Mater Studiorum Università di Bologna Archivio istituzionale della ricerca

Influence of different set-up parameters on the bond behavior of FRM composites

This is the final peer-reviewed author's accepted manuscript (postprint) of the following publication:

*Published Version:*

Influence of different set-up parameters on the bond behavior of FRM composites / Bellini A.; Aiello M.A.; Bencardino F.; de Carvalho Bello C.B.; Castori G.; Cecchi A.; Ceroni F.; Corradi M.; D'Antino T.; De Santis S.; Fagone M.; de Felice G.; Leone M.; Lignola G.P.; Napoli A.; Nistico M.; Poggi C.; Prota A.; Ranocchiaro G.; Realfonzo R.; Sacco E.; Mazzotti C.. - In: CONSTRUCTION AND BUILDING MATERIALS. - ISSN 0950-0618. - ELETTRONICO. - 308:15 November 2021(2021), pp. 124964.1-124964.13. [10.1016/j.conbuildmat.2021.124964]

This version is available at: <https://hdl.handle.net/11585/837783> since: 2021-11-10

*Published:*

DOI: <http://doi.org/10.1016/j.conbuildmat.2021.124964>

*Terms of use:*

Some rights reserved. The terms and conditions for the reuse of this version of the manuscript are specified in the publishing policy. For all terms of use and more information see the publisher's website.

(Article begins on next page)

This item was downloaded from IRIS Università di Bologna (<https://cris.unibo.it/>).  
When citing, please refer to the published version.

# INFLUENCE OF DIFFERENT SET-UP PARAMETERS ON THE BOND BEHAVIOR OF FRCM COMPOSITES

Alessandro Bellini<sup>1,\*</sup>, Maria Antonietta Aiello<sup>2</sup>, Francesco Bencardino<sup>3</sup>, Claudia Brito de Carvalho Bello<sup>4</sup>, Giulio Castori<sup>5</sup>, Antonella Cecchi<sup>4</sup>, Francesca Ceroni<sup>6</sup>, Marco Corradi<sup>5,7</sup>, Tommaso D'Antino<sup>8</sup>, Stefano De Santis<sup>9</sup>, Mario Fagone<sup>10</sup>, Gianmarco de Felice<sup>9</sup>, Marianovella Leone<sup>2</sup>, Gian Piero Lignola<sup>11</sup>, Annalisa Napoli<sup>12</sup>, Mattia Nisticò<sup>3</sup>, Carlo Poggi<sup>8</sup>, Andrea Prota<sup>11</sup>, Giovanna Ranocchiali<sup>10</sup>, Roberto Realfonzo<sup>12</sup>, Elio Sacco<sup>11</sup>, Claudio Mazzotti<sup>13</sup>

<sup>1</sup> CIRI Buildings and Construction (CIRI-EC),  
University of Bologna, Via del Lazzaretto 15/5, 40131, Bologna, Italy

<sup>2</sup> Department of Engineering for Innovation  
University of Salento, Via per Monteroni, 73100 Lecce, Italy

<sup>3</sup> Department of Civil Engineering,  
University of Calabria, Via P. Bucci Cubo 39B, 87036 Rende, Cosenza, Italy

<sup>4</sup> IUAV University of Venice, Dorsoduro 2206, 30123 Venice, Italy

<sup>5</sup> Department of Engineering,  
University of Perugia, Via Duranti 93, 06125 Perugia, Italy

<sup>6</sup> Engineering Department,  
University of Naples 'Parthenope', Centro Direzionale, is. C4, 80143, Napoli, Italy

<sup>7</sup> Department of Mechanical and Construction Engineering,  
Northumbria University, Wynne Jones Building, NE1 8ST Newcastle upon Tyne, United Kingdom

<sup>8</sup> Department of Architecture, Built environment, and Construction Engineering (DABC),  
Politecnico di Milano, Piazza Leonardo da Vinci 32, 20133, Milano, Italy

<sup>9</sup> Department of Engineering,  
Roma Tre University, Via Vito Volterra 62, 00146, Rome, Italy

<sup>10</sup> Department of Civil and Environmental Engineering (DICEA),  
University of Florence, Via di S. Marta 3, 50139, Florence, Italy

<sup>11</sup> Department of Structures for Engineering and Architecture,  
University of Naples 'Federico II', Via Claudio 21, 80125, Napoli, Italy

<sup>12</sup> Department of Civil Engineering  
University of Salerno, Via Giovanni Paolo II 132, 84084 Fisciano, Italy

<sup>13</sup> Department of Civil, Chemical, Environmental and Materials Engineering (DICAM),  
University of Bologna, Viale Risorgimento 2, 40136, Bologna, Italy

\* Corresponding Author

Tel: +39 (0) 51 2090553, email: alessandro.bellini5@unibo.it

## **ABSTRACT**

Fabric Reinforced Cementitious Matrix (FRCM) composites represent an innovative and effective retrofitting solution for masonry structures. The use of FRCMs as an external retrofitting technique requires an insight knowledge of their mechanical behavior, failure modes and masonry-to-FRCM bond properties. A Round Robin Test (RRT) programme was launched by twelve Italian Universities, aimed at evaluating the effect of the shear test set-up parameters and at assessing the test variability. The experimental tests were performed on systems made of glass and steel fibers/cords applied onto masonry substrates. The results were carefully analyzed discussing failure modes, bond capacity, and slip statistical dispersion. Differences in the set-up, including the clamping method, textile impregnation, and instrumentation used for measuring the slip during the tests, were discussed in detail providing useful considerations and suggestions for reducing experimental scattering and obtaining reliable results.

**KEYWORDS:** FRCM; Round Robin; bond test; set-up; experimental scattering

## **1. INTRODUCTION**

Inorganic-matrix composites are an effective solution for the external strengthening of existing masonry structures. They consist of open-mesh textiles made, amongst others, by carbon, glass, aramid, or PBO (p-phenylene-2,6-benzobisoxazole) fiber bundles or unidirectional textiles of steel cords, embedded within inorganic matrices. Amongst the several acronyms used in the literature to indicate these composites, the most common are Fabric Reinforced Cementitious Matrix (FRCM), Textile Reinforced Mortar (TRM), Inorganic Matrix composite Grid (IMG) and, when comprising steel textiles, Steel Reinforced Grout (SRG). Although still considered innovative, they were developed over 20 years ago [1-6] to exploit the high strength-to-weight ratio showed by Fiber Reinforced Polymers (FRP) [7,8] while overcoming the drawbacks of organic matrices. The use of inorganic mortars (lime, cement) instead of organic resins (epoxy, polyester, etc.) entails for a better behavior at high temperatures, easier installation on uneven and wet surfaces, absence of toxic volatile components, and, when the matrix is lime-based, better vapor permeability and compatibility with masonry substrates.

The effectiveness of FRCM composites was experimentally demonstrated in both reinforced concrete [9-17] and masonry [18-36] applications. It was also proven by the significant industrial

developments, which made a large number of strengthening systems available on the construction market and installed in the field, especially in earthquake prone areas, for post-earthquake rehabilitation, and for the retrofitting of architectural heritage [37]. Finally, the recently issued qualification [38,39] and design [40,41] guidelines further confirmed the suitability of FRCM systems for structural rehabilitation and improved the possibility of a standardized control of the whole process, from the production and certification of the products to their acceptance and application in the construction site.

Despite the knowledge gathered and the literature published on the various aspects of structural rehabilitation of masonry structures with FRCM, the bond properties still remain one of the most crucial issues. This is because the effectiveness of the strengthening solution relies on the load transfer capacity between the member and the externally bonded reinforcement. The study of the bond behavior is complicated by the wide range of existing FRCM systems and constituent materials, by the multiple failure modes that can occur, complex interaction between textile, matrix, and substrate, brittle behavior of mortar matrices, and by the influence of installation and curing conditions. Therefore, further research is still necessary to improve the knowledge on bond behavior (capacity, failure mode) and test methods, which proved to be crucial for the bond characterization and the identification of FRCM design properties [42]. These issues were already widely tackled in the past (see, amongst others [43-53]). A systematic investigation was carried out in a previous RRT [54-56], which involved some of the institutions that also carried out this work. In that case, the amount of data available for one specific FRCM system was limited by the large number of reinforcements under study. Additionally, although some general instructions were shared before the RRT, experimental set-ups significantly differed from each other. Finally, each laboratory took care of the construction of its own masonry substrate prisms and of the installation of the reinforcements.

For the specific purpose of investigating the masonry-to-FRCM bond in detail and further contributing to the state of knowledge, a specific RRT was launched within the ReLUIIS research

project, which involves the Italian Network of Earthquake Engineering Laboratories and is funded by the Italian Civil Protection Department. Shear bond tests were carried out on three FRCM systems, two of which comprised of bidirectional alkali-resistant glass textiles (named Glass 1 and Glass 2) and the remaining one made of an unidirectional textile of galvanized ultra-high tensile strength steel (UHTSS) cords (named Steel). In all cases, the matrices were lime mortars and the FRCM systems were bonded to substrate prisms made by clay bricks and lime mortar joints.

Twelve Italian Universities took part to the initiative: Universities of Bologna, Calabria, Cassino, Florence, Naples “Federico II”, Naples “Parthenope”, Perugia, Politecnico di Milano, Roma Tre, Salento, of Salerno and Venice (IUAV). Each laboratory carried out five shear bond tests on FRCM Glass 1, Glass 2, or Steel (Table 1). Each system was tested by more laboratories (from 6 to 9) to allow comparisons and get robust statistics. In order to reduce the variability associated with manufacturing, all the specimens strengthened with Glass 1 system were prepared (i.e. the masonry prisms were built and cured, and the FRCM strips were bonded and cured) by the Politecnico di Milano and all the specimens with the others two systems were prepared by the University of Bologna. After manufacturing and curing, the specimens were shipped to the participants for testing. As for experimental set-ups, all tests were carried out using a single-lap test arrangement and the RILEM TC-250 recommendations [57] were followed, to have the same (basic) test conditions. Testing machines, load and displacement transducers, and small details in equipment (e.g. gripping method, steel frames) and testing procedures (e.g. load rate, pre-load), in addition to the operators who performed the test, differed from laboratory to laboratory. In this paper, the outcomes of the RRT are analyzed to obtain information on the inherent variability of shear bond test results, on the effects of set-up implementation, such as equipment details and measurement techniques and to identify reliable values of experimental scattering correlated with this type of tests and materials, associated both to the activity of one single lab or to a number of them. This will be useful to set acceptance criteria in future or existing guidelines on this aspect.

## 2. EXPERIMENTAL PROGRAM AND MATERIALS MECHANICAL PROPERTIES

The experimental program focuses on the evaluation of the effects of different set-up parameters on the bond behavior of three types of FRCM retrofitting systems applied on masonry substrate and on the variability of bond capacity (i.e. peak applied load divided by the fiber cross-sectional area) expected when performing single-lap shear tests on these materials. Samples were tested by 12 different Italian Universities, within a Round-Robin Test (RRT) activity, according to the experimental arrangement summarized in Table 1, where the three FRCM systems (Glass 1, Glass 2 or Steel) were associated to the Universities (UNI) where tests were conducted. Five test repetitions for each strengthening system were performed.

### 2.1. FRCM components

The three different FRCM systems consisted of balanced glass fiber grids (Glass 1 and Glass 2) or unidirectional steel fiber cords (Steel) embedded in lime mortars.

The Glass 1 strengthening system (see Figure 1a) was comprised of a styrene-butadiene rubber (SBR) coated glass fiber grid with an area weight density (including the coating) of  $360 \text{ g/m}^2$  (equivalent dry fiber thickness = 0.05 mm) and a nominal spacing of 18 mm. The matrix was a lime mortar with a compressive strength of 22 MPa and a flexural strength of 6 MPa (values declared by the manufacturer).

The Glass 2 system (Figure 1b) was comprised of an uncoated glass fiber grid with a spacing of 16 mm and an area weight density of  $300 \text{ g/m}^2$  (equivalent dry fiber thickness = 0.06 mm), which was embedded within the matrix after the application of an adhesion promoter, used for improving adhesion between fibers and mortar [48,49]. The matrix was a fiber-reinforced lime mortar, containing short glass fibers, characterized by a compressive strength of 10.56 MPa and a flexural strength of 3.75 MPa [58].

The third system (Figure 1c) was comprised of a unidirectional reinforcement made of galvanized ultra-high strength steel (UHTSS) micro-cords, with an area weight density of  $670 \text{ g/m}^2$  and an

equivalent dry fiber thickness of 0.084 mm. The dark color lines in Figure 1c identify the UHTTS cords of the strengthening system, whereas the light color mesh is a secondary non-structural grid, used for maintaining the position of the steel cords and preserve the shape of the reinforcement during the application, which has negligible mechanical properties. This system was applied with a lime mortar with a compressive strength of 14.81 MPa and a flexural strength of 3.27 MPa [58].

The tensile properties of the textile and of the FRCM systems were evaluated by means of tensile tests performed both on dry fibers [59] and on FRCM coupons [39]. Test results on dry fibers are reported in Table 2, where, for each strengthening system, the mean tensile strength and elastic modulus are given together with their coefficient of variation (CoV). Samples used for both uniaxial tensile and shear tests had the same number of yarns (or cords) (4 yarns for Glass 1 and Glass 2, 8 cords for Steel), in order to allow a direct comparison, as the number of yarns (or cords) was found to have an impact on results [53].

FRCM systems were mechanically characterized, as also suggested by the Italian Guidelines [39], by means of tensile tests on coupons made by using a width ( $w$ ) chosen as an integer multiple of the spacing between yarns (74 mm for Glass 1, 64 mm for Glass 2, 50 mm for Steel) and an overall length of 500 mm. Composite tabs were applied at the ends of the samples in order to avoid stress concentration due to machine clamping.

Results of FRCM characterization are shown in Figure 2 in terms of fiber stress-strain curves, whereas the main mechanical parameters are presented in Table 3. This table also reports the stress values corresponding to the transition between different branches and elastic moduli of the first un-cracked phase and of the final branch are reported. The tensile stresses are referred to the cross-sectional area of dry fibers only, whereas the strains were obtained by extensometers applied to the specimens central area, using a 200 mm gage length. By using the clamping-grip method described in [44], three branches can be generally identified in the stress-strain response. The stresses  $\sigma_{T1}$ ,  $\sigma_{T2}$ , and  $\sigma_u$  identify the transition from the first to the second branch, from the second to the third one, and the tensile strength of the coupon, respectively. The slopes of the first (un-cracked) and of the

final branches of the stress-strain curves were calculated using the letter designation  $E_1$  and  $E_3$ , respectively.

Glass 2 and Steel coupons did not show a clear second branch of the stress-strain curve. Glass 2 samples, because of the addition of the adhesion promoter that entailed for a better matrix-fiber stress transfer, provided a continuous transition between the different branches and their behavior could be described by a bilinear function rather than by the typical tri-linear one [48]. Similarly, a reliable identification of the second (cracked) branch of the Steel system was difficult since the cracking phase was characterized by the development of numerous distributed micro-cracks. Therefore, values of  $\sigma_{T2}$  are not reported in Table 3 for Glass 2 and Steel systems.

As an additional remark, while for Glass 2 and Steel specimens a smooth transition between the first and second branch was observed, stress-strain curves of Glass 1 showed several load drops after the end of the first branch due to the occurrence of matrix cracks. The stress redistribution among the fiber yarns after the opening of a matrix crack depends on the randomly distributed matrix-fiber bond properties, which in turn affect the stress-strain response. Indeed, scattered results are often observed in inorganic-matrix composites [52].

## **2.2. Substrate properties and geometry**

The three FRCM systems (Glass 1, Glass 2 and Steel) were applied on the same masonry substrate, made with standard clay solid bricks (with nominal dimensions  $250 \times 120 \times 55 \text{ mm}^3$ ) and a lime mortar. Each masonry prism was realized with 5 stacked clay bricks and 4 mortar bed joints, with a thickness of approximately 10 mm, obtaining samples with nominal dimensions  $250 \times 120 \times 315 \text{ mm}^3$  (see Figure 3a). FRCM systems were applied without any specific surface preparation except for cleaning, brushing and wetting the surface with a cloth. Bricks were mechanically characterized by means of compression tests on 50 mm diameter core-drilled cylindrical samples, obtaining an average compressive strength of 18.63 MPa and a splitting tensile strength of 2.60 MPa. Mechanical properties of the lime mortar used for bedding were measured by means of sample tests

[58], obtaining an average compressive and flexural strength of 3.72 MPa and 1.52 MPa, respectively.

### 3. TEST SET-UPS

The single-lap push-pull scheme (see Figure 3*b,c*) was used for bond tests by the different laboratories. This test arrangement is suggested by RILEM TC-250 recommendations [57]: the sample is located inside a rigid steel frame, able to prevent displacements and rotations. All the samples were characterized by the same FRCM bonded length (260 mm). The bonded width ( $w$  in Figure 3*a*) of each FRCM sample was chosen as an integer multiple of the spacing between yarns (see Sect. 2.1). A 30 mm long area of the FRCM strengthening systems (measured from the front side of the masonry prism) was left unbonded, and a mortar thickness of 6 mm for Glass 2 and Steel samples and of 10 mm for Glass 1 specimens were used. During samples preparation, a portion of the textile strip was left bare, without any type of impregnation. Only for Glass 2 samples, the unbonded portion of the FRCM was later impregnated with epoxy resin following different procedures (single yarns impregnation or textile impregnation), as discussed in the following. Composite or aluminum tabs were applied at the end of the bare textile strip before connecting samples to the clamping system of the testing machine. The relative displacement between textile and substrate (*slip*) was measured by means of different types of displacement transducers (LVDTs, potentiometers, draw-wire displacement transducers (WDTs)), by using as reference point on the FRCM a steel or aluminum profile glued to the bare textile in correspondence of the beginning of the unbonded part and as reference on the substrate points close to the former (Figure 3*b*).

Some laboratories applied a slight pre-tension load before performing the tests, in order to achieve a proper alignment of the yarns.

All bond tests were performed in displacement control by adopting a stroke displacement rate in the range 0.10 – 0.50 mm/min, which includes typical displacement rates used for testing inorganic-matrix composites. The loading rate may affect the bond behavior of FRCM composites [60].

However, the differences in the loading rate adopted in the round robin campaign were assumed to be small and their effect was neglected.

Similarities and differences between the test set-ups used by the different Universities were summarized in Table 4 for the three types of FRCM systems tested, in terms of testing machine capacity, clamping method, instrumentation used for measuring the slip, and displacement test rate (see also Figure 4). In the following sections, a description of the main differences characterizing the set-ups used to test each type of strengthening system is reported.

### **3.1. Glass 1 tests**

Details of experimental set-ups used for single-lap shear tests on Glass 1 samples are reported in Table 4. Universal testing machines with load capacity in the range 100 – 500 kN were employed, except for UNI 1, which used a machine with larger capacity. Direct hydraulic clamping was used in the majority of the set-ups, while in few cases other systems were used. In particular, UNI 6 clamped the specimens using two steel plates bolted together and adding also glue to ensure firm clamping. A spherical joint connected the bolted steel plates to the testing machine. The use of bolted steel plates does not generally allow for preventing the fiber-matrix slippage within the clamped area and this, along with the presence of spherical joints, may cause an uneven distribution of the applied force among the textile yarns. A similar effect can also be caused by the use of clamping wedges without the possibility to control the gripping pressure. The effect of these different clamping methods will be analyzed in detail during the discussion of the experimental results.

The textile-substrate slip was always measured using two LVDTs with a 10 mm or 20 mm measuring range, with the exception of UNI 1, which employed two wire displacement transducers (WDTs with 750 mm gage length). The use of WDTs is not recommended since the relative displacements are very smalls and WDT are mostly used in cases of large displacements. Their use could lead to a low accuracy and scattered results. Glass 1 samples were tested without any

additional impregnation of the unbonded textile (note that the glass textile was coated). Bond tests were performed under displacement control with similar test rates (0.10 – 0.25 mm/min range), except for UNI 1 (test rate equal to 0.50 mm/min), as shown in Table 4.

### **3.2. Glass 2 tests**

Glass 2 samples were comprised of a bare glass fiber grid impregnated by an adhesion promoter before being embedded within the lime mortar. Uneven distribution of tensile force among the specimen width was observed in bare fiber yarns and textiles, since they have a reduced capacity of stress redistribution among fiber filaments and among yarns [53,61]. Before performing the bond tests, depending on the laboratory, the single yarns (SY in Table 4) or the entire textile (T in Table 4) of the unbonded part were impregnated with epoxy resin. Preliminary bond tests carried out by UNI 2 without impregnation of the unbonded textile confirmed that the uneven applied load redistribution led to small bond capacities and scattered results, with a failure mode involving the premature local tensile rupture of the dry fibers along the unbonded part of the textile (Figure 5). These tests provided an average bond capacity 67% smaller than that obtained from specimens with impregnated unbonded textile.

The clamping method used by the different laboratories included both hydraulic and mechanical clamping, with the main differences coming from UNI 6 and UNI 8 set-ups; they employed two steel plates bolted (UNI 6) or epoxy glued (UNI 8) together, connected to the grips of the testing machine by a spherical joint. Concerning samples instrumentation, as for Glass 1 specimens, LVDTs were used in most of the cases, except for UNI 1 (WDTs with 750 mm gage length). All the tests were carried out under displacement control with the same crosshead speed used for Glass 1 specimens. In particular, Table 4 shows similar crosshead speeds (0.10 – 0.25 mm/min range) for all laboratories, except for UNI 1 and UNI 8 (crosshead speed equal to 0.50 mm/min).

### **3.3. Steel tests**

Experimental set-ups used for Steel specimens were similar, with small modifications between laboratories. Even if different types of tabs were used (aluminum or composite materials bonded with epoxy resin), specimens were clamped using hydraulic or mechanical clamping methods without the use of spherical or cylindrical joints, thus leading to a similar load transferring mechanism. Concerning instrumentation and test rates (see Table 4), the differences among laboratories were small since LVDTs and potentiometers were used and displacement rates were in the range 0.10 – 0.25 mm/min. The high standardization of the experimental set-ups, together with the absence of sudden load drops due to matrix cracking, are key parameters to be taken into account for discussing and understanding experimental results on Steel samples and their statistical variability.

## **4. EXPERIMENTAL RESULTS**

Experimental results coming from single-lap shear tests performed on glass and steel FRCM systems will be reported and discussed in the following sub-sections in terms of failure modes, bond capacity and stress-slip curves.

### **4.1. Bond failure modes**

Failure modes observed during single-lap shear tests were reported in Tables 5-7, respectively, for Glass 1, Glass 2, and Steel samples and shown in detail in Figure 6. They were labeled by a letter designation (A to F), according to the classification proposed in [39], which was reported also in Table 5, with a brief description.

Table 5 showed that the most common failure mode observed during bond tests on Glass 1 samples was the tensile failure of the composite grid outside of the bonded area (failure mode F, see Figure 6*d*), with only a few cases of mixed failure modes involving both slippage of the textile within the

matrix with cracking of the outer mortar layer (E) and final tensile failure of the textile (F), observed in some specimens tested by UNI 10.

Glass 2 specimens (see Table 6) showed only a single failure mode (F), already detected in Glass 1 specimens, confirming that this mechanism is typical of relatively low density glass fiber textiles coupled with cementitious or lime based mortars [48,49], where the good adhesion between matrix and substrate generally allows to fully exploit the tensile capacity of the textile.

Even if the impregnation was made after the application of FRCM and potentially the impregnation of the dry fibers at the extremity of the unbonded part of the textile was not optimal, no failure occurred close to that portion. Moreover, the low density of these textiles determines tensile failure loads of the FRCM reinforcement associated to tensile rupture of the fibers that are comparable or lower than the tensile loads associated with the achievement of the interface bond strength.

Since Glass 1 and Glass 2 are different systems, a direct comparison between them is not possible and is beyond the scope of this paper. However, as a general remark, as long as the adhesion provided by FRCM matrices is appropriate (which is the present case), it is generally frequent to reach the maximum tensile strength of the textile. For what concerns the contribution of the adhesion promoter used in Glass 2 samples, further details can be found in [48,49].

Steel samples presented several failure mechanisms (Table 7), with a predominance of failure mode C (debonding at the textile-to-matrix interface, see Figure 6c), but also some cases of tensile rupture of the textile (failure mode F), occurring at high levels of load. Sometimes, such as for UNI 4, UNI 6, and UNI 9, failure mode C occurred together with a partial debonding at the matrix-to-substrate interface (B+C, see Figure 6b) or, in a single case, a complete detachment from the masonry substrate occurred (failure mode B for UNI 11, see Figure 6a). Mixed failure mechanisms (C+E) were detected during bond tests performed at UNI 7 and UNI 12, with the latter laboratory including also single cases of C+F or C+E+F mechanisms.

The explanation of the observed failure modes lies in the fact that steel cords have higher tensile strengths in comparison to glass fibers and, for this reason, the limiting factor is the adhesion at the

different interfaces; this aspect, as highlighted by other experimental studies [56], made often possible debonding failure mechanisms before reaching the ultimate tensile capacity of the reinforcement. For this reason, most of the Steel samples showed failure mode C (debonding at the textile-to-matrix interface) with a bond capacity obviously lower than the maximum tensile strength of steel cords.

#### **4.2. Stress-slip envelopes and bond capacity**

The envelopes of experimental stress-slip curves obtained from bond tests were reported in Figure 7. The stress was calculated considering the cross-sectional area of the dry fibers (without including the matrix), whereas the slip was the average of the displacements measured by the two LVDTs, potentiometers, or WDTs placed at the beginning of the FRCM unbonded part (see Figure 3).

Each envelope includes the five curves provided by each laboratory for a given strengthening system. Figure 7*a* and *b* show the stress-slip envelopes obtained from Glass 1 and Glass 2, respectively. Due to the high number of laboratories involved, results of bond tests on Steel system were split into two figures (Figure 7*c* and Figure 7*d*), providing in both figures the indication of the limits of the global envelope (i.e. the envelope of all the stress-slip curves of Steel samples – black line).

From a first qualitative evaluation of the shape of the curves, it can be noticed that both Glass 1 and Glass 2 samples showed a similar brittle behavior without any softening, consistent with the most common identified failure mode (tensile failure of the textile), sometimes with load drops corresponding to the tensile rupture of the single yarns [54].

Steel samples, due to different failure modes (debonding at the textile-to-matrix interface or mixed mechanisms) showed generally a more pronounced nonlinear behavior, with a larger displacement capacity after the first peak and before final failure. In case of debonding phenomena, the shape of the stress-slip curves was characterized by typical pseudo-horizontal branches.

The comparison of the stress-slip envelopes in Figure 7a and b showed that the use of WDTs led to higher slip measurements than those measured with LVDTs.

The average bond capacity  $\sigma_{f,max,m}$  (i.e. maximum applied load divided by the cross-sectional area of the fibers) of the three different strengthening systems were reported in Tables 5-7 for Glass 1, Glass 2, and Steel samples, respectively, along with the corresponding CoV. These tables also report the average slip  $Slip_m$  associated with the peak stress and the corresponding CoV. Slip at peak stress showed significantly higher scatter than the bond capacity. Therefore, it should be not considered as a reliable parameter for describing the results of single-lap shear tests.

## **5. DISCUSSION OF EXPERIMENTAL RESULTS**

In the following, experimental outcomes will be analyzed in terms of bond capacity and slip variability among the different laboratories, in order to obtain useful indications on the expected scattering of results.

The most relevant effects of set-up parameters and samples preparation on the results will be discussed, providing practical recommendations for set-up standardization that may help reducing the overall results variability.

### **5.1. Bond capacity**

When considering results from Glass 1 samples (Table 5), the low performances recorded by UNI 6 may be attributed to the differences in the experimental set-up with respect to other laboratories (UNI 2, UNI 3, UNI 5 and UNI 10). Due to the use of the spherical joints, the clamping pressure could not be controlled and this caused a different stress distribution among the yarns, in comparison to direct grip clamping. The adoption of the same experimental set-up for Glass 2 samples caused again a low performance of specimens tested at UNI 6 (see Table 6). This confirmed that the use of direct grip clamping with a controlled clamping pressure should be preferred when performing bond tests on glass specimens or more in general on FRCM systems

characterized by low fibers density. An alternative method could involve the use of very thick and rigid plates with an adequate clamping. Table 6 also shows that single yarn impregnation is less effective than textile impregnation with epoxy resin in redistributing stresses along the free part of the textile, as confirmed by the higher results obtained by UNI 2 and UNI 3 with respect to others. This result can be explained considering the capability of textile impregnation to redistribute the applied force among fiber filaments and yarns, whereas impregnation of single yarns does not allow for redistributing the applied load among different yarns.

Bond capacity results coming from single-lap shear tests on Steel samples are reported in Table 7 where, despite the numerous failure modes detected, a smaller dispersion of results can be observed, due to the limited differences in the experimental set-ups.

Bond capacity results, except for Glass samples which manifested tensile rupture of the textile, could be compared with theoretical predictions coming from the literature, in case of debonding failure mechanisms [62]. In fact, Eq. (2) proposed in [62] provides a theoretical formulation for assessing the maximum strain as a function of the axial stiffness of the reinforcement and of the mechanical properties of masonry substrate. Using results coming from mechanical characterization, a bond capacity of 921 MPa can be estimated. However, since detachment in Steel samples usually occurs at the textile-to-matrix interface (failure mode C) and since the theoretical formulations do not explicitly include this failure mechanism, a further improvement is possible using matrix mechanical properties instead of those of masonry substrate, obtaining a predicted bond capacity of 1626 MPa, with a lower underestimation of experimental results.

## **5.2. Dispersion of bond capacity results**

The bond capacity  $\sigma_{f,max}$  of each specimen is shown in Figure 8 with respect to the different laboratories. Figure 8 provides a first overview of the variability of results within the same laboratory and a comparison also with the whole experimental dataset, expressed in terms of average value (dashed red line) and 95% confidence interval (shaded area), determined according to

Annex D of EN 1990 [63]. The results show that dealing with a mean bond capacity obtained averaging results from different laboratories can be misleading. Systematic errors and poor repeatability of results from some laboratory can lead to over- or under-estimation of the performance of the system. This can happen even under the best technical circumstances and should be considered by taking into account the randomly distributed properties of inorganic-matrix composites. In order to minimize this aspect, a strict standardization of the test procedure is necessary.

Figure 8 also shows the average tensile strengths of the FRCM system ( $\sigma_{f,max,FRCM}$ ) and the dry textile strength ( $\sigma_{f,max,textile}$ ), indicated with dashed lines, in order to evaluate the exploitation ratio  $\eta_{FRCM}$  of the strengthening systems with respect to the FRCM capacity, defined as  $\eta_{FRCM} = \sigma_{f,max} / \sigma_{f,max,FRCM}$ . The use of the tensile strength value of the FRCM system to calculate the exploitation ratio instead of the tensile strength of the dry textile, was made in order to take into account the interaction between fibers and mortar, considering the whole composite system and not only one of its components. For the glass systems,  $\eta_{FRCM}$  is in the range 60-70%, while for the steel system an average  $\eta_{FRCM} = 85\%$  was obtained.

A representation of the bond capacity dispersion coming from different laboratories is presented in Figure 9, where the CoV of the three FRCM materials, referred to tests from each laboratory, were reported in the form of histograms, together with reference lines corresponding to the CoV of the whole dataset for each system. The Steel system showed the smallest dispersion, with a CoV of 18.2% for the entire dataset (see Table 7 and Figure 9), followed by Glass 2 system (CoV = 20.2%, see Table 6) and Glass 1 system (CoV = 27.3%, see Table 5). When considering the average of the CoVs from each laboratory, the smallest values are 14.4%, 14.3%, and 16.1% for Glass 1, 2, and Steel systems respectively. Comparison among these numbers indicated that the large scattering of results from the whole dataset can be attributed not only to usual data dispersion observed in inorganic-matrix composites but also to some systematic differences introduced by the laboratories (further details can be found in section 5.4). In the case of the Steel system, dispersion of results

considering the whole dataset or the average of the CoVs is similar, since this systematic influence by specific laboratories cannot be found. At the same time, these CoVs could have been even lower, but they were increased by the contribution from some laboratories which experienced different failure modes of the specimens, such as cords tensile failure or matrix-to-substrate debonding, leading to the highest and lowest strength values (Figure 8). This did not happen so clearly for other systems, where consistent failure modes led to values more uniformly scattered among the laboratories.

### **5.3. Slip statistical variation**

In addition to bond capacity, another parameter evaluated during single-lap shear tests was, as already discussed, the relative displacement (slip) between the beginning of the unbonded portion of the textile and the adjacent masonry substrate. Starting from each stress-slip experimental curve, the slip value corresponding to the maximum stress was considered and the mean value  $Slip_m$  calculated for each type of FRCM system and for each testing laboratory. Results were reported in Tables 5-7, together with the corresponding CoVs. If the statistical variation of this parameter for each laboratory is analyzed, CoV is included in the range 17.0 - 60.7% for Glass 1 system, 11.4% to 63.6% for Glass 2 system, and 10.3 - 87.4% for Steel system. The CoV calculated by considering the whole dataset was 78.7% for Glass 1, 55.8% for Glass 2, and 34.1% for Steel systems. The high statistical variability of  $Slip_m$  suggested that, while the bond capacity was a significant parameter generally affected by an acceptable variation, slip at peak stress was not always reliable for the interpretation of bond test results, since it strongly depended on the failure mode and local behavior of the stress-slip curve.

#### **5.4. Effect of set-up parameters and samples preparation on the bond capacity**

In this section, starting from the discussion of experimental outcomes, the main effects of different set-up parameters and sample preparation methods are analyzed, obtaining useful recommendations for the standardization of the test procedure.

##### *5.4.1 Clamping method*

The preferred clamping methods during the RRT activity presented were characterized by the application of composite or aluminum tabs with epoxy resin at the end of the specimen unbonded textile and by the adoption of controlled hydraulic or mechanical grips. The use of alternative methods, such as those based on steel bolted plates, with or without spherical or cylindrical connections to the machine, proved to be a not efficient method because, generally, the poor and uncontrolled clamping pressure caused non-uniform slippage of the yarns in the unbonded part of the specimens and a consequent non-effective redistribution of the tensile force among them, leading to a premature tensile failure of the textile. This phenomenon, extremely significant in brittle materials, was particularly noticed on Glass 1 samples tested at UNI 6, leading to an evident and rather systematic low bond capacity and it was also confirmed by tests on Glass 2 specimens by the same laboratory. As previously discussed, the use of steel plates instead of direct grip clamping could be an alternative only if plates are very thick and rigid (undeformable) and coupled with an effective clamping method.

##### *5.4.2 Instrumentation*

The instrumentation used for measuring the slip included different types of displacement transducers (LVDTs, potentiometers, and WDTs). LVDTs were preferred by most of the laboratories and proved to be the optimal choice in terms of both sensitivity and reliability, especially if used with an appropriate (10 or 20 mm) measuring range. Alternative instruments, such as potentiometers and wire displacement transducers showed more scattered results, due to their

lower sensitivity in measuring very small displacements, often leading to an incorrect determination of the slope of the initial branch of stress-slip curves. For this reason, LVDTs with 10 mm or 20 mm measuring ranges seem to be the most appropriate solution for specimen instrumentation.

#### *5.4.3 Textile impregnation*

Samples preparation also played a key role for obtaining repeatable and reliable results. While the Steel system did not require a specific preparation of the unbonded part of the textile, the same did not apply for brittle materials, such as glass or basalt fiber textiles. This is particularly the case of uncoated fibers (Glass 2 samples). Indeed, preliminary bond tests performed on Glass 2 specimens, without any preparation of the unbonded part, showed that only a minimal part of the bond capacity (approximately 37% of the capacity obtained after textile impregnation) could be achieved. In the case of coated fibers (Glass 1 system), the effect is still present, but less relevant with respect to the previous one. The impregnation by epoxy resin proved to be most effective in the case of application to the whole unbonded textile, while it showed lower results in the case of application to single yarns only. The analysis of experimental outcomes showed that textile impregnation was effective in promoting the even distribution of applied force among fiber filaments and yarns and in reducing the experimental scattering, as highlighted by the results obtained by UNI 2 and UNI 3 on Glass 2 samples (see Table 6).

### **5.5. Recommendations (for set-up standardization)**

Results of bond tests on FRCM samples showed that a set-up standardization is needed for obtaining reliable results and limiting the experimental scatter. Tests should always be performed in displacement control, since the FRCM system can exhibit softening or pseudo-horizontal branches in case of debonding phenomena. Results may be affected by the test control method (displacement or force), the clamping method and clamping pressure, the preparation of the unbonded part of the textile and by the instrumentation used. The bond tests carried out during this experimental program

showed that testing methods other than direct grip clamping (using a controlled clamping pressure) are not recommended since they can cause a high and non-uniform slippage of the textile inside the clamping device, with premature failures. On the contrary, methods based on direct grip clamping and on the application of composite or aluminum tabs through epoxy at the free end of the specimen have to be preferred since they provided the best results in terms of bond capacity.

The preparation of the unbonded part of the textile has an effect on the structural behavior of brittle materials, such as glass, carbon, or basalt fiber textiles. Experimental results demonstrated that full textile impregnation is the recommended method, in order to allow a uniform force redistribution between yarns and avoid premature brittle failures outside of the bonded area. As an additional recommendation, the application of a light pre-tension load to the yarns before applying epoxy resin or before the single-lap shear test (within the range 2-5% of the maximum fabric tensile strength), is important to achieve a better alignment and to facilitate a uniform distribution of the force between them.

Concerning samples instrumentation, LVDTs proved to be the best choice, thanks to their high sensitivity and reliability, for measuring the slippage of the textile and obtaining reliable stress-slip curves. Other types of displacement transducers, such as potentiometers or WDTs, are not recommended and could cause significant errors in the determination of the system initial stiffness. Despite the use of LVDTs, the slip at peak was found to be a non-reliable parameter, strongly dependent on the failure mode and on local variations of the stress-slip curve, especially in the case of pseudo-horizontal branches of the curve, such as during delamination phenomena (Figure 7c,d). Adoption of these recommendations in current procedures and guidelines for bond tests on FRCM systems could improve the reliability and repeatability of results.

## **6. CONCLUSIONS**

This paper presented the results of a Round Robin Test organized within the ReLUIIS research project and involved twelve Italian Universities. The test programme was focused on the evaluation

of the influence of different set-up parameters on the bond behavior of three FRCC systems and on the corresponding bond capacity variability.

Experimental outcomes confirmed the expected failure modes of the FRCC strengthening systems tested which, according to previous RRT activities, included tensile rupture of the textile for glass-based FRCC composites and more complex mechanisms (debonding at the textile-to-matrix-interface, debonding at the textile-to-substrate interface, fiber slippage or tensile failure of the textile) for steel-based composites.

Furthermore, the results obtained allowed for drawing the following main conclusions:

- Clamping method and textile impregnation along the unbonded portion significantly affected the bond behavior of FRCC with brittle fibers. Namely, the use of spherical joints promoted a non-uniform stress redistribution among the longitudinal fiber yarns. Similarly, impregnation of single longitudinal yarns did not allow for a proper stress redistribution across the composite width. Direct grip clamping, with a controlled hydraulic pressure and unbonded part preparation (possibly using full textile impregnation) are the recommended methods, especially for brittle materials, since local effects of defects (e.g. heterogeneous stretching of the fibers) are amplified on the global response and experimental bond capacity due to progressive failure of the different yarns.
- The slip at peak load cannot be considered as a reliable parameter and should not be used as a reference for certification activities, because its value strongly depends on specific test setup, especially on the position of the displacement transducers.
- The RRT activity indicated that a coefficient of variation (CoV) of the bond capacity in the 15-20% range can be realistically expected by an experimental program carried out by a single laboratory. A higher CoV could suggest a poor control of test conditions or invalid failure modes. In order to make these values applicable on a technical basis, a strict standardization of the experimental set-up is needed.

Outcomes of the presented work could provide a significant contribution to the improvement of test procedures implemented in current FRCM qualification guidelines, with the aim of reaching a high level of standardization and reducing experimental scattering related to small but not negligible differences in experimental set-ups.

## **7. ACKNOWLEDGEMENTS**

The financial support of the Italian Department of Civil Protection (ReLUIIS 2019-21 Grant – Innovative Materials) is gratefully acknowledged. The authors would like to thank Sika Italia S.p.A., Fibre Net S.p.A and Kerakoll S.p.A. for providing materials and for the cooperation during samples preparation.

## REFERENCES

- [1] Curbach M, Jesse F. High-performance textile-reinforced concrete. *Structural Engineering International* 1999;9:289-291.
- [2] Briccoli Bati S, Rotunno T. A composite material in glass-fiber and cement-matrix (GFRCM) for masonry reinforcement. *Fifth international symposium on computer methods in structural masonry*, Rome, Italy, 18-21 April 2001, ed. T. G. Hughes, G. N. Pande Swansea: Computers & Geotechnics 2001 pp. 181-189, ISBN 9780951038024.
- [3] Briccoli Bati S, Rotunno T. GFRCM and CFRP composite materials in masonry reinforcement. *Proceedings of Ninth International Conference on Composites Engineering, ICCE/9*, Denver, 2002.
- [4] Briccoli Bati S, Feletti I, Rotunno T. Reinforcement with GFRCM of structural masonry elements: experimental studies of in scale models. *Proceedings of the International Conference Composites in Constructions*, Cosenza, Italy, 16-19 September 2003, pp. 165-170, ISBN: 88-7740-358-6.
- [5] Huang X, Birman V, Nanni A, Tunis G. Properties and potential for application of steel reinforced polymer and steel reinforced grout composites. *Composites Part B* 2005;36:73-82.
- [6] Triantafillou TC, Papanicolaou CG. Shear strengthening of reinforced concrete members with textile reinforced mortar (TRM) jackets. *Material and Structures* 2006;39(285):93-103.
- [7] Guadagnini M, Serbescu A, Palmieri A, Matthys S, Bilotta A, Nigro E, Ceroni F, Czadersky C, Olia S, Szambo Z, Balazs G, Mazzotti C. Round Robin Test on the bond behaviour of externally bonded FRP systems to concrete. *Proc. of 6th International Conference on FRP Composites in Civil Engineering (CICE 2012)*, Rome, Italy, 13-15 June 2012, CD ROM.
- [8] Savoia M, Bilotta A, Ceroni F, Di Ludovico M, Fava G, Ferracuti B, Mazzotti C, Nigro E, Olivito R, Pecce M, Poggi C. Experimental round robin test on FRP concrete bonding. *Proc. of FRP RCS9*, Sydney, Australia, 13-15 July 2009, CD ROM.
- [9] D'Ambrisi A, Focacci F. Flexural strengthening of RC beams with cement based composites. *Journal of Composites for Construction* 2011;15(2):707-20.
- [10] Ombres L. Flexural analysis of reinforced concrete beams strengthened with a cement based high strength composite material. *Composite Structures* 2011;94(1):143-55.
- [11] Hashemi S, Al-Mahaidi R. Experimental and finite element analysis of flexural behavior of FRP-strengthened RC beams using cement-based adhesives. *Construction and Building Materials* 2012;26:268-73.
- [12] Babaeidarabad S, Loreto G, Nanni A. Flexural strengthening of RC beams with an externally bonded fabric-reinforced cementitious matrix. *Journal of Composites for Construction* 2014;18(5):1-12.
- [13] Sneed LH, Verre S, Carloni C, Ombres L. Flexural behavior of RC beams strengthened with steel-FRCM composite. *Engineering Structures* 2016;127:686-99.
- [14] Loreto G, Babaeidarabad S, Leardini L, Nanni A. RC beams shear-strengthened with fabric-reinforced-cementitious-matrix (FRCM) composite. *International Journal of Advanced Structural Engineering* 2015;7:341-52.

- [15] Napoli A, Realfonzo R. Reinforced concrete beams strengthened with SRP/SRG systems: Experimental investigation. *Construction and Building Materials* 2015;93:654-677.
- [16] Gonzalez-Libreros JH, Sabau C, Sneed LH, Pellegrino C, Sas G. State of Research on Shear Strengthening of RC Beams Using FRCM Composites. *Construction and Building Materials* 2017;149:444-458.
- [17] Larrinaga P, Garmendia L, Piñero I, San-José JT. Flexural strengthening of low-grade reinforced concrete beams with compatible composite material: Steel Reinforced Grout (SRG). *Construction and Building Materials* 2020;235:117790.
- [18] Papanicolaou CG, Triantafillou TC, Papathanasiou M, Karlos K. Textile reinforced mortar (TRM) versus FRP as strengthening material of URM walls: out-of-plane cyclic loading. *Materials and Structures* 2008;41(1):143-157.
- [19] Papanicolaou CG, Triantafillou TC, Lekka M. Externally bonded grids as strengthening and seismic retrofitting materials of masonry panels. *Construction and Building Materials* 2011;25(2):504-515.
- [20] Borri A, Casadei P, Castori G, Hammond J. Strengthening of brick masonry arches with externally bonded steel reinforced composites. *Journal of Composites in Construction* 2009;13(6):468-475.
- [21] Faella C, Martinelli E, Nigro E, Paciello S. Shear capacity of masonry walls externally strengthened by a cement-based composite material: An experimental campaign. *Construction and Building Materials* 2010;24:84-93.
- [22] Harajli M, Elkhatib H, San-Jose T. Static and cyclic out-of-plane response of masonry walls strengthened using textile-mortar system, *Journal of Materials in Civil Engineering* 2010;22(11):1171-1180.
- [23] D'Ambrisi A, Feo L, Focacci F. Experimental and analytical investigation on bond between Carbon-FRCM materials and masonry. *Composites Part B* 2013;46:15-20.
- [24] Razavizadeh A, Ghiassi B, Oliveira DV. Bond behavior of SRG-strengthened masonry units: Testing and numerical modeling. *Construction and Building Materials* 2014;64:387-397.
- [25] Babaeidarabad S, De Caso F, Nanni A. Out-of-Plane Behavior of URM Walls Strengthened with Fabric-Reinforced Cementitious Matrix Composite, *Journal of Composites for Construction* 2014;18(4),04013057.
- [26] Valluzzi MR, Da Porto F, Garbin E, Panizza M. Out-of-plane behavior of infill masonry panels strengthened with composite materials. *Materials and Structures* 2014;47(12):2131-2145.
- [27] Fossetti M, Minafò G. Strengthening of Masonry Columns with BFRCM or with Steel Wires: An Experimental Study. *Fibers* 2016;4(2):15.
- [28] Mezrea PE, Yilmaz IA, Ispir M, Binbir E, Bal IE, Ilki A. External Jacketing of Unreinforced Historical Masonry Piers with Open-Grid Basalt-Reinforced Mortar. *Journal of Composites for Construction* 2016;21(3),04016110.
- [29] Bellini A, Incerti A, Bovo M, Mazzotti C. Effectiveness of FRCM Reinforcement Applied to Masonry Walls Subject to Axial Force and Out-Of-Plane Loads Evaluated by Experimental and Numerical Studies. *International Journal of Architectural Heritage* 2018;12(3):376-394.

- [30] D'Ambra C, Lignola GP, Prota A, Sacco E, Fabbrocino F. 2018. Experimental performance of FRCC retrofit on out-of-plane behaviour of clay brick walls. *Composites Part B* 2018; 148:198-206.
- [31] Minafò G, La Mendola L. Experimental investigation on the effect of mortar grade on the compressive behaviour of FRCC confined masonry columns. *Composites Part B* 2018;146:1-12.
- [32] Ombres L, Verre S. Masonry columns strengthened with Steel Fabric Reinforced Cementitious Matrix (S-FRCC) jackets: experimental and numerical analysis. *Measurement* 2018;127:238-245.
- [33] De Santis S, De Canio G, de Felice G, Meriggi P, Roselli I. Out-of-plane seismic retrofitting of masonry walls with Textile Reinforced Mortar composites. *Bulletin of Earthquake Engineering* 2019;17(11):6265-6300.
- [34] de Carvalho Bello CB, Boem I, Cecchi A, Gattesco N, Oliveira DV. Experimental tests for the characterization of sisal fiber reinforced cementitious matrix for strengthening masonry structures, *Construction and Building Materials* 2019;219:44-55.
- [35] De Santis S. Bond behaviour of Steel Reinforced Grout for the extrados strengthening of masonry vaults. *Construction and Building Materials* 2017;150:367-382.
- [36] Torres B, Ivorra S, Baeza FJ, Estevan L, Varona B. Textile reinforced mortars (TRM) for repairing and retrofitting masonry walls subjected to in-plane cyclic loads. An experimental approach. *Engineering Structures* 2021;231:111742.
- [37] Belliazzi S, Ramaglia G, Lignola GP, Prota A. Out-of-Plane Retrofit of Masonry with Fiber-Reinforced Polymer and Fiber-Reinforced Cementitious Matrix Systems: Normalized Interaction Diagrams and Effects on Mechanisms Activation. *Journal of Composites for Construction* 2021;25(1).
- [38] ICC-ES. AC434 Acceptance criteria for masonry and concrete strengthening using fiber-reinforced cementitious matrix (FRCC) composite systems. ICC-Evaluation Service, Whittier, CA, USA, 2016.
- [39] CSLLPP (Italian Council for Public Works). Linee Guida per la identificazione, la qualificazione ed il controllo di accettazione di compositi fibrorinforzati a matrice inorganica (FRCC) da utilizzarsi per il consolidamento strutturale di costruzioni esistenti. 2019.
- [40] ACI 549 0L – RILEM TC 250-CSM. ACI 549.6R-2020: Guide to design and construction of externally bonded Fabric-Reinforced Cementitious Matrix (FRCC) and Steel-Reinforced Grout (SRG) systems for repair and strengthening masonry structures. ISBN: 978-1-64195-120-3.
- [41] CNR (Italian National Research Council). CNR-DT 215/2018: Guide for the design and construction of Externally Bonded Fibre Reinforced Inorganic Matrix systems for strengthening existing structures. 2020.
- [42] De Santis S, Hadad HA, De Caso y Basalo FJ, de Felice G, Nanni A. Acceptance Criteria for Tensile Characterization of Fabric Reinforced Cementitious Matrix (FRCC) Systems for Concrete and Masonry Repair. *Journal of Composites for Construction* 2018;22(6):04018048.
- [43] D'Antino T, Carloni C, Sneed LH, Pellegrino C. Matrix-fiber bond behavior in PBO FRCC composites: A fracture mechanics approach. *Engineering Fracture Mechanics* 2014;117:94-111.

- [44] Carozzi FG, Poggi C. Mechanical properties and debonding strength of Fabric Reinforced Cementitious Matrix (FRCM) systems for masonry strengthening. *Composites Part B* 2015;70:215-230.
- [45] Bilotta A, Ceroni F, Nigro E, Pecce M. (2017). Experimental tests on FRCM strengthening systems for tuff masonry elements, *Construction and Building Materials* 2017;138:114-133.
- [46] Ceroni F, Salzano P. Design provisions for FRCM systems bonded to concrete and masonry elements. *Composites Part B* 2018;143:230-242.
- [47] Grande E, Imbimbo M, Sacco E. Numerical investigation on the bond behavior of FRCM strengthening systems. *Composites Part B* 2018;145:240-251.
- [48] Bellini A, Bovo M, Mazzotti C. Experimental and numerical evaluation of fiber-matrix interface behaviour of different FRCM systems. *Composites Part B* 2019;161:411-426.
- [49] Bellini A, Shahreza SK, Mazzotti C. Cyclic bond behavior of FRCM composites applied on masonry substrate. *Composites Part B* 2019;169:189-199.
- [50] Ascione F, Lamberti M, Napoli A, Realfonzo R. Experimental bond behavior of Steel Reinforced Grout systems for strengthening concrete elements. *Construction and Building Materials* 2020;232:1-13.
- [51] Carozzi FG, Arboleda D, Poggi C, Nanni A. Direct Shear Bond Tests of Fabric-Reinforced Cementitious Matrix Materials. *Journal of Composites for Construction* 2020;24(1),4019061.
- [52] de Felice G, D'Antino T, De Santis S, Meriggi P, Roscini F. Lessons learned on the tensile and bond behaviour of Fabric Reinforced Cementitious Matrix (FRCM) composites. *Frontiers in Built Environment, section Earthquake Engineering* 2020;6:5.
- [53] Bilotta A, Lignola GP. Effect of fiber-to-matrix bond on the performance of inorganic matrix composites. *Composite Structures* 2021;265,113655.
- [54] Leone M, Aiello MA, Balsamo A, Carozzi FG, Ceroni F, Corradi M, Gams M, Garbin E, Gattesco N, Krajewski P, Mazzotti C, Oliveira D, Papanicolaou C, Ranocchiai G, Roscini F, Saenger D. Glass fabric reinforced cementitious matrix: Tensile properties and bond performance on masonry substrate. *Composites Part B* 2017;127:196-214.
- [55] Caggegi C, Carozzi FG, De Santis S, Fabbrocino F, Focacci F, Hojdys L, Lanoye E, Zuccarino L. Experimental analysis on tensile and bond properties of PBO and aramid fabric reinforced cementitious matrix for strengthening masonry structures. *Composites Part B* 2017;127:175-195.
- [56] De Santis S, Ceroni F, de Felice G, Fagone M, Ghiassi B, Kwiecień A, Lignola GP, Morganti M, Santandrea M, Valluzzi MR, Viskovic A. Round Robin Test on tensile and bond behaviour of Steel Reinforced Grout systems. *Composites Part B: Engineering*, 2017;127:100-120.
- [57] de Felice G, Aiello MA, Caggegi C, Ceroni F, De Santis S, Garbin E, Gattesco N, Hojdys Ł, Krajewski P, Kwiecień A, Leone M, Lignola GP, Mazzotti C, Oliveira DV, Papanicolaou C, Poggi C, Triantafyllou T, Valluzzi MR, Viskovic A. Recommendation of RILEM TC 250-CSM: Test method for Textile Reinforced Mortar to substrate bond characterization. *Materials and Structures* 2018;51(4):95.
- [58] UNI-EN 1015-11. Methods of test for mortar for masonry – Part 11: Determination of flexural and compressive strength of hardened mortar. 2007.

- [59] EN 2561. Aerospace series – Carbon fibre reinforced plastics – Unidirectional laminates – Tensile test parallel to the fibre direction. 1995.
- [60] Carloni C, Verre S, Snel LH, Ombres L. Loading rate effect on the debonding phenomenon in fiber reinforced cementitious matrix-concrete joints. *Composites Part B* 2017;108:301-314.
- [61] D’Antino T, Poggi C. Stress redistribution in glass fibers of G-FRCM composites. *Key Eng Mater* 2019;817:520-527.
- [62] Ceroni F, Salzano P. Design provisions for FRCM systems bonded to concrete and masonry elements. *Composites Part B* 2018;143:230-242.
- [63] EN 1990:2002/A1:2005. Eurocode – Basis of structural design. 2005.

**Table 1.** Experimental program: FRCM systems and universities involved.

University	System 1 Glass 1	System 2 Glass 2	System 3 Steel
UNI 1	×	×	
UNI 2	×	×	×
UNI 3	×	×	×
UNI 4			×
UNI 5	×	×	
UNI 6	×	×	×
UNI 7	×		×
UNI 8		×	
UNI 9			×
UNI 10	×		×
UNI 11			×
UNI 12			×

**Table 2.** Tensile properties of dry textiles.

Material	Number of tests	Tensile strength		Young's modulus	
		Mean	CoV	Mean	CoV
		[MPa]	[%]	[GPa]	[%]
Glass 1	5	968	3.7	68.1	2.2
Glass 2	5	1131	3.1	65.0	1.4
Steel	5	3184	0.8	200.9	0.9

**Table 3.** Results of tensile tests on FRCM strengthening systems.

FRCM	# of tests	Tensile strengths			Elastic moduli			
		$\sigma_{T1}$	$\sigma_{T2}$	$\sigma_u$	$E_1$	$E_3$		
Glass 1	4	Mean [MPa]	329	330	1028	Mean [GPa]	680.3	62.2
		CoV [%]	9.7	10.9	9.6	CoV [%]	19.2	5.8
Glass 2	5	Mean [MPa]	130	-	1096	Mean [GPa]	413.3	60.9
		CoV [%]	2.3	-	2.5	CoV [%]	19.0	1.2
Steel	5	Mean [MPa]	73	-	2857	Mean [GPa]	542.5	193.5
		CoV [%]	15.5	-	2.0	CoV [%]	23.4	4.2

**Table 4.** Experimental set-ups.

University	FRCM	Universal testing machine capacity [kN]	Clamping method	Instrumentation	Textile (unbonded part)	Test rate [mm/min]
UNI 1	Glass 1	1200	Composite tabs, hydraulic clamping	2 WDTs (750 mm)	N	0.50
	Glass 2				SY	
UNI 2	Glass 1	250	Epoxy tabs, hydraulic clamping	2 LVDTs (20 mm)	N	0.20
	Glass 2				T	
	Steel				N	
UNI 3	Glass 1	100	Epoxy tabs, hydraulic clamping	2 LVDTs (20 mm)	N	0.10
	Glass 2		Composite tabs, hydraulic clamping		T	
	Steel		Epoxy tabs, hydraulic clamping		N	
UNI 4	Steel	100	Epoxy tabs, mechanical clamping	2 LVDTs (20 mm)	N	0.20
UNI 5	Glass 1	500	Aluminium tabs + epoxy, hydraulic clamping	2 LVDTs (10 mm)	N	0.25
	Glass 2				SY	
UNI 6	Glass 1	300	Steel plates + bolts, ball joint	2 LVDTs (20 mm)	N	0.15
	Glass 2				SY (external only)	
	Steel		Epoxy tabs, mechanical clamping		N	
UNI 7	Glass 1, Steel	500	Aluminium tabs + epoxy, hydraulic clamping	2 LVDTs (10 mm)	N	0.25
UNI 8	Glass 2	125	Steel plates + epoxy resin, vertical hinge	2 LVDTs (20 mm)*	SY	0.50
UNI 9	Steel	250	Composite tabs, mechanical clamping	2 LVDTs (50 mm)	N	0.25
UNI 10	Glass 1, Steel	500	Aluminium tabs + two-component adhesive, hydraulic clamping	2 LVDTs (10 mm)	N	0.18
UNI 11	Steel	630	Epoxy tabs, hydraulic clamping	2 Potentiometers (50 mm)	N	0.20
UNI 12	Steel	100	Steel tabs + epoxy, mechanical clamping	2 LVDTs (10 mm)	N	0.20

N = no impregnation

SY = single yarn impregnation with epoxy resin

T = textile impregnation with epoxy resin

\* = applied on the matrix at the beginning of the bonded part

**Table 5.** Glass 1: experimental results.

University	$\sigma_{f,max,m}$ [MPa]	CoV [%]	Slip <sub>m</sub> ( $\sigma_{f,max}$ ) [mm]	CoV [%]	Failure mode
UNI 1	590	23.0	1.52	60.7	F
UNI 2	698	14.6	0.98	41.2	F
UNI 3	624	8.0	0.34	27.2	F
UNI 5	815	18.4	2.62	30.4	F
UNI 6	367	13.6	0.41	31.6	F
UNI 7	478	9.1	0.50	22.9	F
UNI 10	740	14.2	1.62	17.0	E+F(2), F(3)
<b>Whole dataset</b>	<b>608</b>	<b>27.3</b>	<b>1.05</b>	<b>78.7</b>	-

A = debonding with cohesive failure of the substrate

B = debonding at the matrix-to-substrate interface

C = debonding at the textile-to-matrix interface

D = textile slippage within the mortar matrix

E = textile slippage within the matrix with cracking of the outer layer of mortar

F = tensile rupture of the textile (outside of the bonded area)

**Table 6.** Glass 2: experimental results.

University	$\sigma_{f,max,m}$ [MPa]	CoV [%]	Slip <sub>m</sub> ( $\sigma_{f,max}$ ) [mm]	CoV [%]	Failure mode
UNI 1	577	21.1	1.17	11.4	F
UNI 2	864	10.0	0.63	43.6	F
UNI 3	867	2.7	0.37	52.6	F
UNI 5	784	24.6	0.39	63.6	F
UNI 6	664	22.8	0.56	37.8	F
UNI 8	800	4.7	-	-	F
<b>Whole dataset</b>	<b>757</b>	<b>20.2</b>	<b>0.64</b>	<b>55.7</b>	-

**Table 7.** Steel: experimental results.

University	$\sigma_{f,max,m}$ [MPa]	CoV [%]	Slip <sub>m</sub> ( $\sigma_{f,max}$ ) [mm]	CoV [%]	Failure mode
UNI 2	2752	7.8	1.77	31.8	C
UNI 3	2245	31.3	1.43	10.3	C(3), F(2)
UNI 4	2130	22.2	2.00	32.2	B+C(1), C(4)
UNI 6	2560	11.7	2.16	37.7	B+C(2), C(3)
UNI 7	2468	18.4	1.61	37.8	C+E(2), C(3)
UNI 9	2235	20.1	2.11	13.4	B+C(2), C(3)
UNI 10	2659	11.5	1.72	22.7	C(4), F(1)
UNI 11	2184	16.2	1.83	12.4	B(1), C(4)
UNI 12	2747	5.9	1.50	87.4	C+E(3), C+F(1), C+E+F(1)
<b>Whole dataset</b>	<b>2430</b>	<b>18.2</b>	<b>1.80</b>	<b>34.1</b>	-

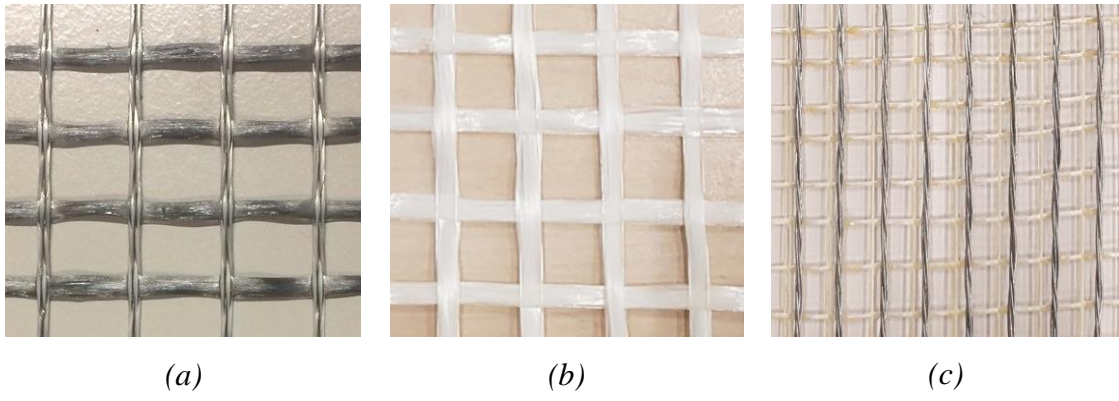
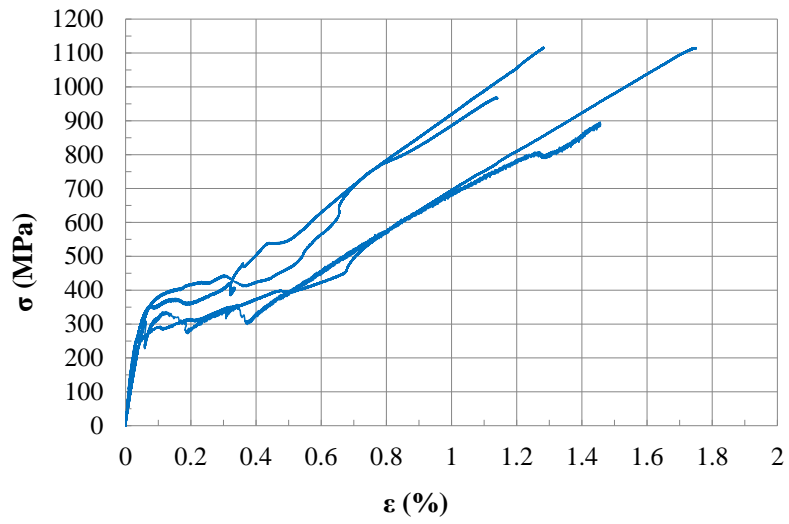
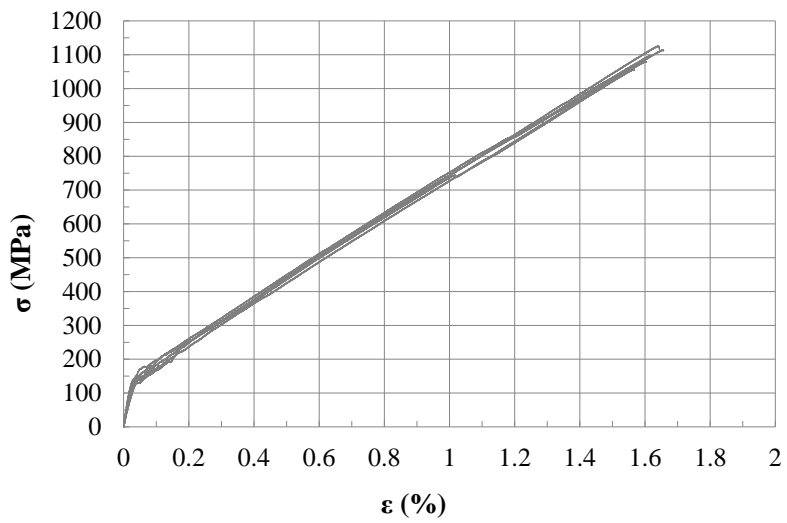


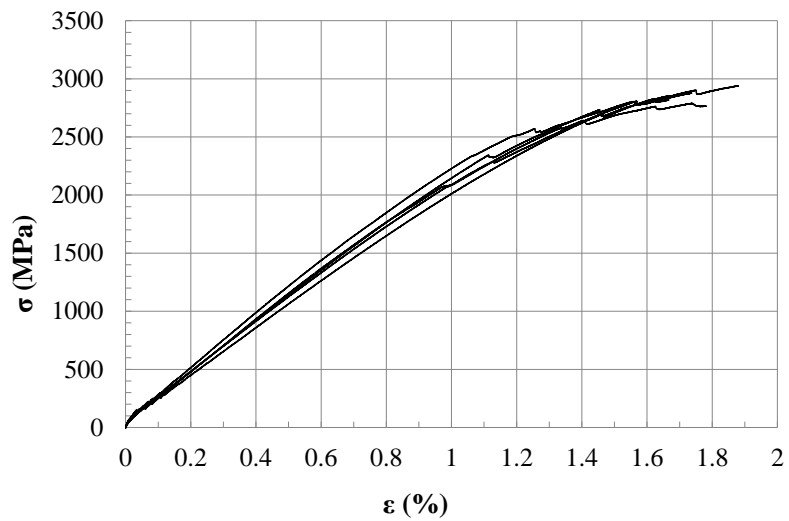
**Figure 1.** Textiles used for the FRCM systems tested: (a) Glass 1; (b) Glass 2; (c) Steel.



(a)



(b)



(c)

**Figure 2.** Tensile behavior of FRCM coupons: (a) Glass 1; (b) Glass 2; (c) Steel.

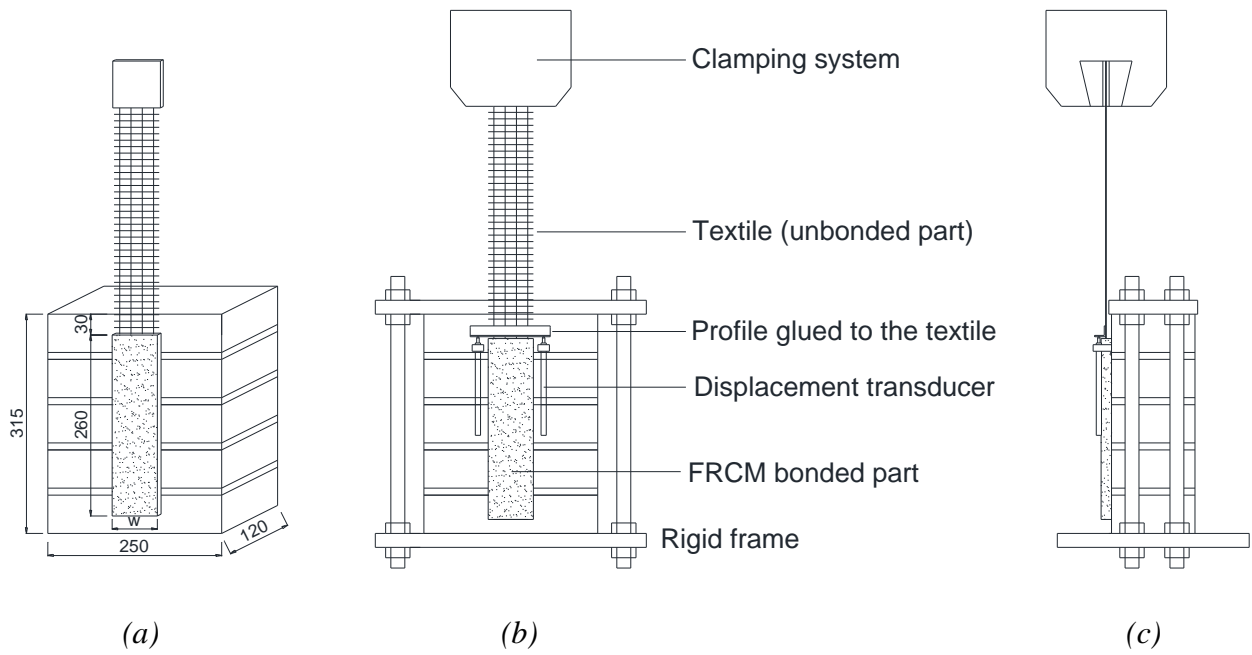
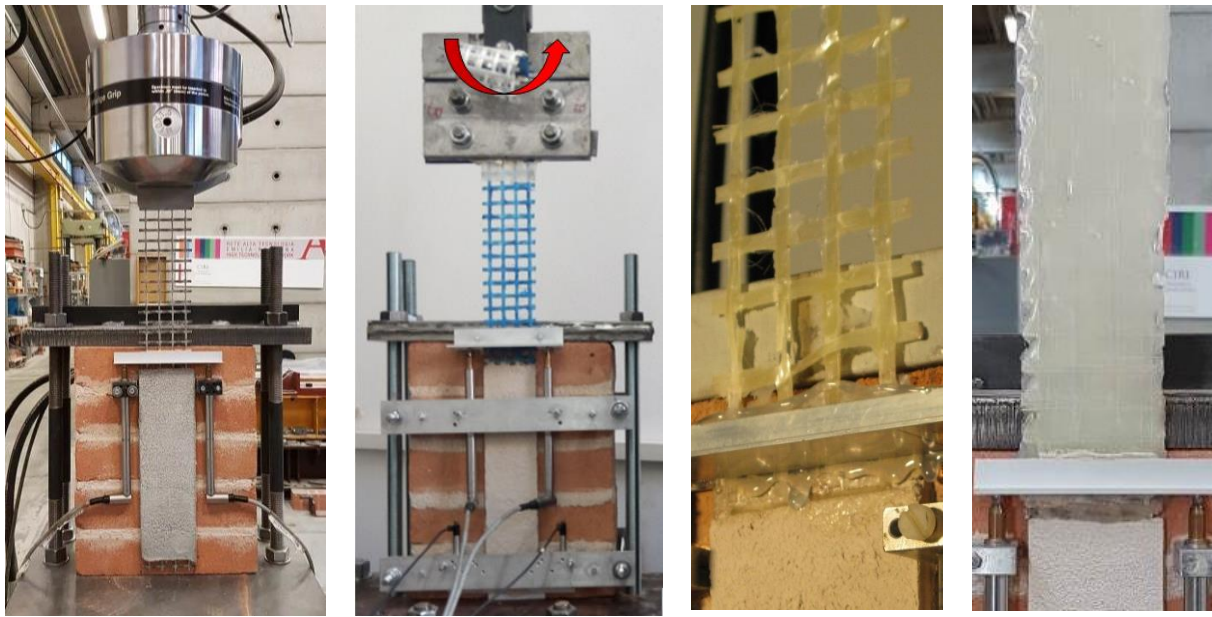


**Figure 3.** Geometry of the samples and experimental set-up (in the specific case of hydraulic clamping): (a) three-dimensional view; (b) front side view; (c) lateral side view.



(a)

(b)

(c)

(d)

**Figure 4.** Examples of clamping methods and textile (unbonded part) preparation: (a) direct hydraulic clamping (with tabs); (b) clamping using steel plates and hinge (ball joint); (c) single yarn impregnation with epoxy resin; (d) full textile impregnation.

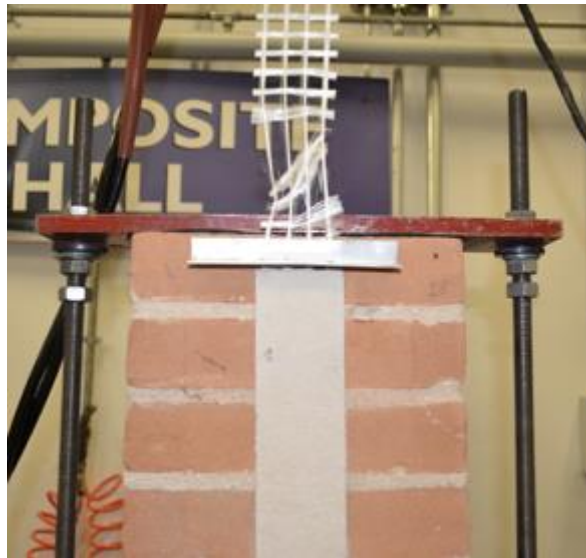


**Figure 5.** Preliminary bond tests on Glass 2 samples without fibers impregnation: premature failure of uncoated glass fibers along the unbonded part of the textile.

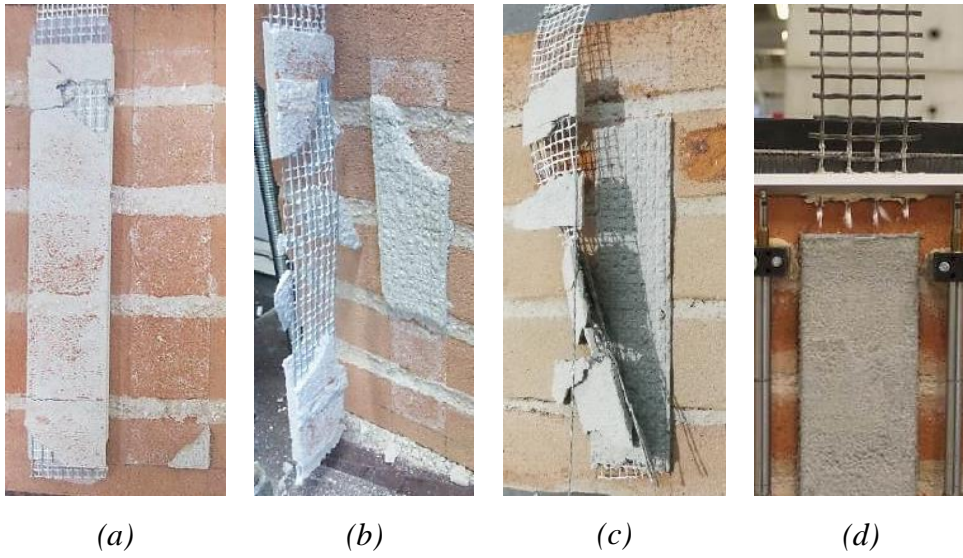
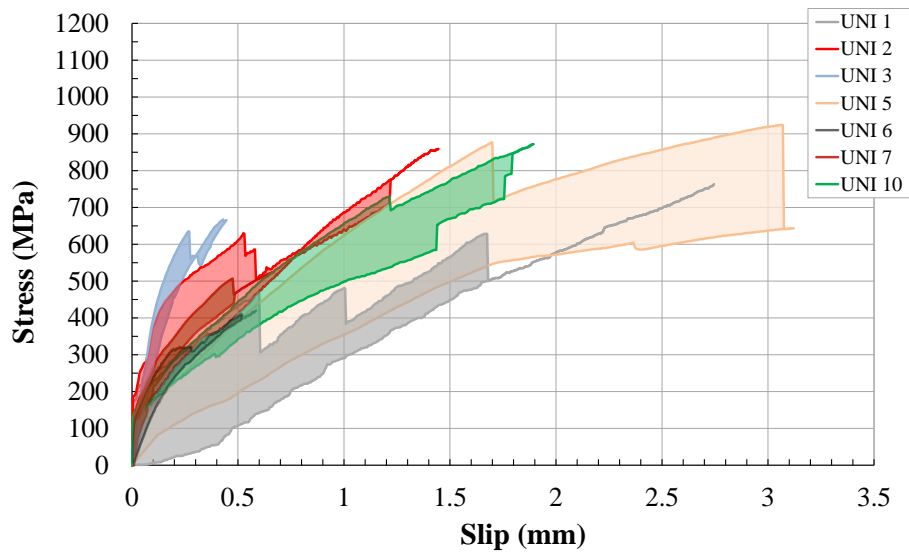
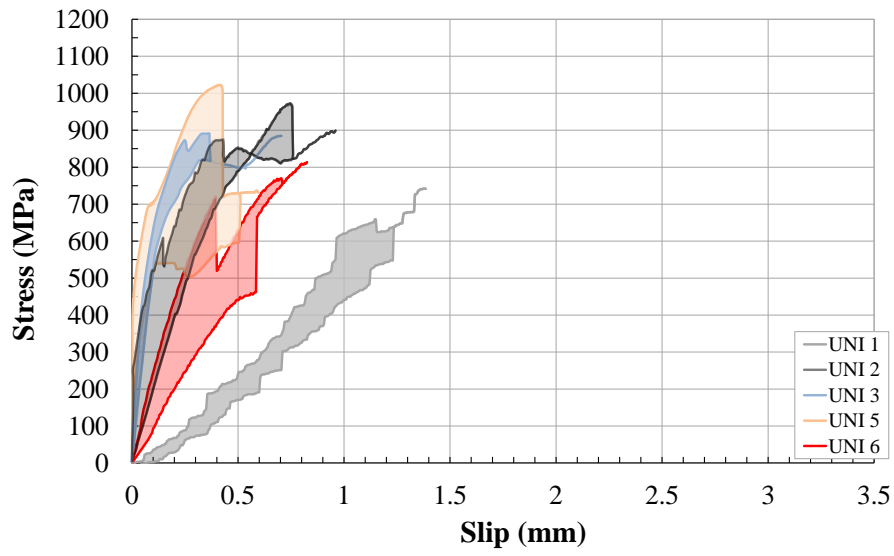


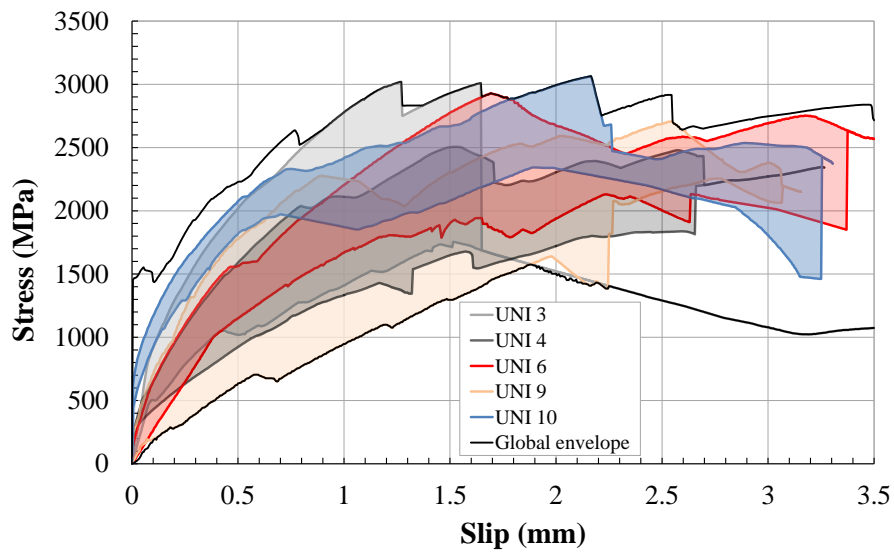
**Figure 6.** Failure modes: (a) B (Steel); (b) B+C (Steel); (c) C (Steel); (d) F (glass).



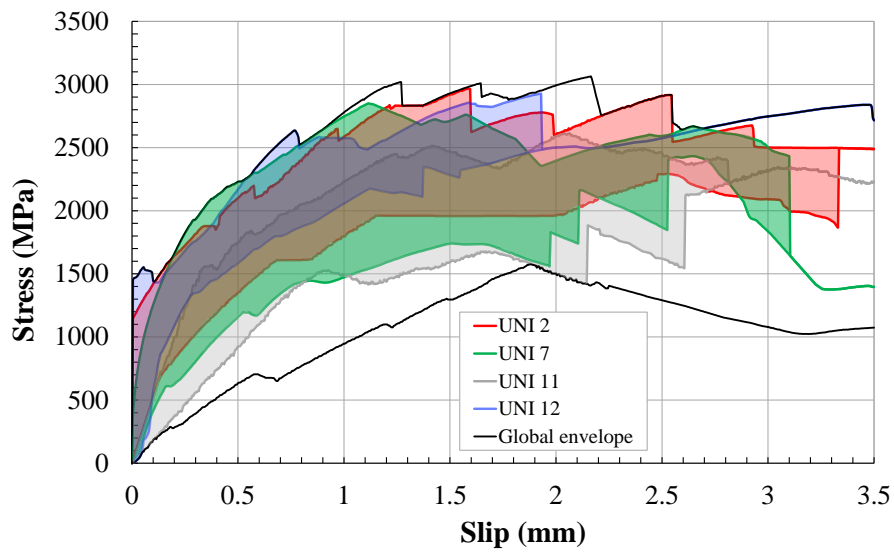
(a)



(b)

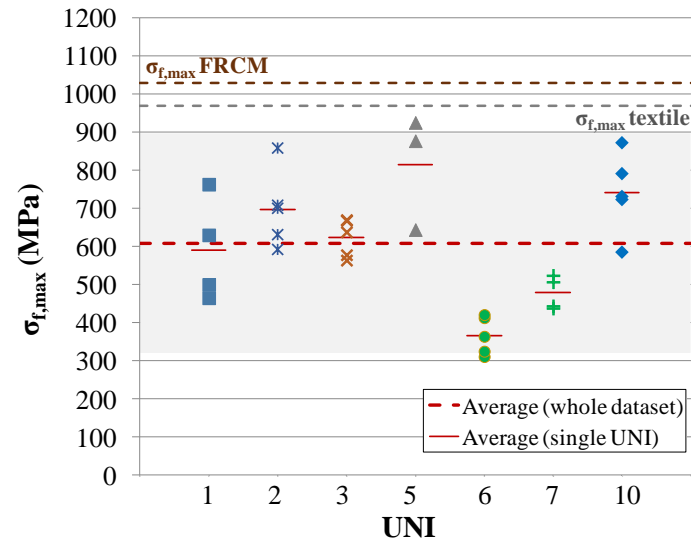


(c)

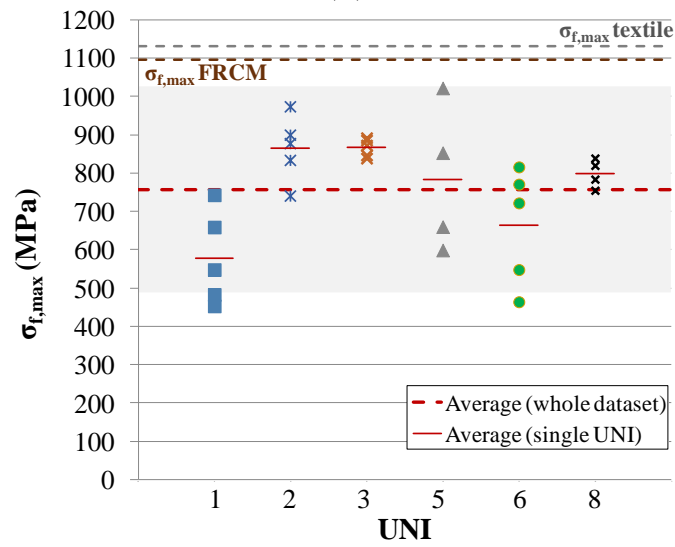


(d)

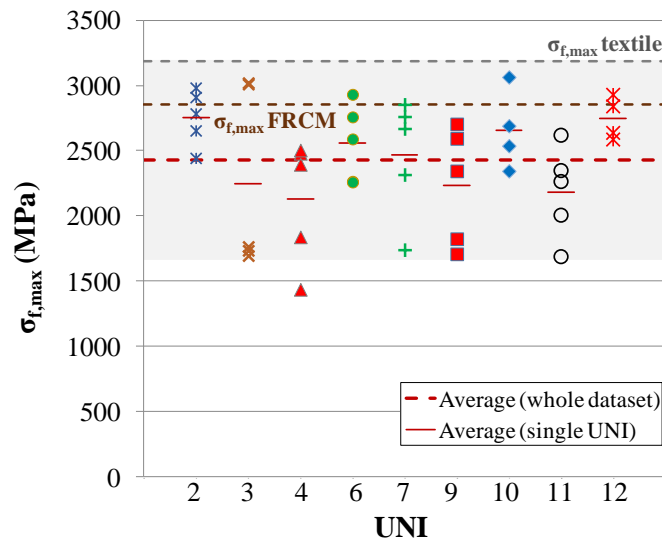
**Figure 7.** Stress-slip envelopes: (a) Glass 1; (b) Glass 2; (c) and (d) Steel.



(a)



(b)



(c)

**Figure 8.** Variation of bond capacity: *a)* Glass 1; *b)* Glass 2; *c)* Steel.

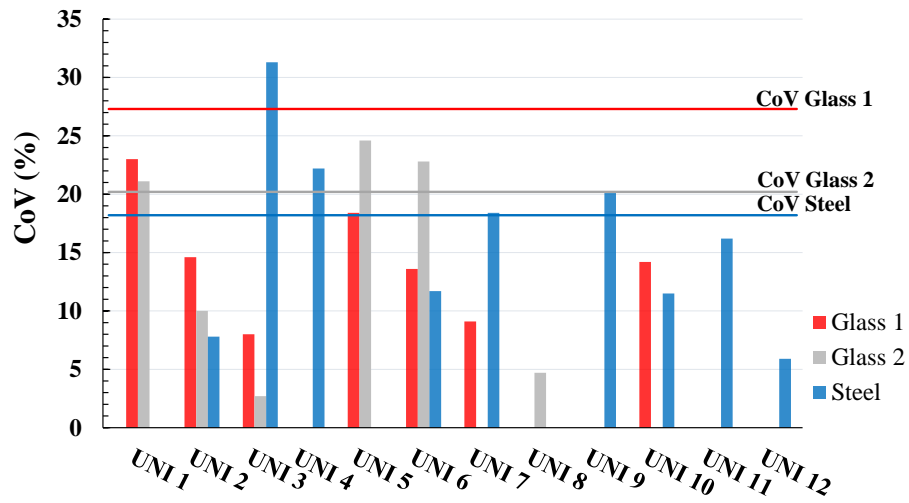


**Figure 9.** Variation of bond capacity: comparison between different laboratories.